

ISSN 1872-2040

Vo1.38

No.11

November

2010

CHINESE JOURNAL OF ANALYTICAL CHEMISTRY

Sponsored by the Chinese Chemical Society
the Chinese Academy of Sciences

<http://www.analchem.cn>

E-mail: fxhx@ciac.jl.cn

Immobilization of Myoglobin on NiO Nanoparticles Matrix for Preparation of Novel Biosensor

ZONG Shui-Zhen¹, CUI Rong-Jing¹, FEI Lei¹, LI Wei-Wei¹, JU Huang-Xian^{2,*}

¹ Department of Chemistry and Material Engineering, Changshu Institute of Technology, Changshu, Jiangsu 215500, China

² School of Chemistry and Chemical Engineering, Nanjing University, Key Lab of Analytical Chemistry for Life Science, Ministry of Education, Nanjing, Jiangsu 210018, China

Abstract: Direct electrochemistry that immobilized myoglobin (Mb) on a nanometer-sized NiO nanoparticles matrix modified graphite electrode (GE) and preparation of novel hydrogen peroxide biosensor were studied. The immobilized Mb displayed a couple of stable and well-defined redox peaks with an electron transfer rate constant of 6.48 s^{-1} and a formal potential of -0.340 V (vs saturated calomel electrode [SCE]) in 0.1 M pH 7.0 PBS. The total surface concentration Γ was $8.06 \times 10^{-10}\text{ mol cm}^{-2}$. Dimethyl sulfoxide (DMSO) could play an important role in the electron transfer between Mb and the electrode. Spectroscopy analysis of the Mb/NiO/DMSO film showed that the immobilized Mb could retain its natural structure. The electrocatalytic response showed a linear dependence on the H_2O_2 concentration ranging from 0.8 to $24\text{ }\mu\text{M}$ with a detection limit of $0.039\text{ }\mu\text{M}$ at 3σ . The apparent Michaelis–Menten constant K_M^{app} for H_2O_2 sensor was estimated to be 0.21 mM , sensitivity was $417\text{ mA/M}\cdot\text{cm}^{-2}$, showing a high affinity.

Key Words: NiO nanoparticles; Biosensors; Hydrogen peroxide; Myoglobin; Direct electron transfer

1 Introduction

The study of protein and enzyme direct electrochemistry and electrocatalysis, for understanding the life of electron transfer mechanism and enzyme-catalyzed mechanism, as well as key life-substance in the life of important redox process is very important^[1]. Recent studies show that the direct electron transfer can be realized between heme proteins and the electrode surface by using the surfactants^[2,3], sol-gel film^[4], ion polymer^[5], nanomaterials^[6–11] by embedding, cross-linking, assembling, and so on. People have more interest in the immobilization of protein (enzyme) molecules in nanoparticle with the in-depth research on nanomaterials^[6,12,13]. Myoglobin (Mb) is the ideal model of direct electrochemistry on

heme proteins, biosensing, and electrocatalytic because it involves the electron delivery in physiological function and the process of metabolism. Nickel oxide as a functional material, many scholars are very much aware on its development and the study of application^[14].

This thesis work is to immobilize myoglobin molecule to nickel oxide nanoparticles (NiO) modified graphite electrode (GE) surface, study the direct electrochemistry behavior of protein (enzyme) in the NiO nanoparticles modified GE for the first time, and design an accurate, reliable, convenient, sensitive new third-generation biosensor with good selectivity, stability, and reproducibility. This research takes on the great theoretical and practical significance in the life sciences, environmental science, energy science, and analytical chemistry.

2 Experimental procedures

Received 18 March 2010; accepted 11 June 2010

* Corresponding author. Email: hxju@nju.edu.cn

This work was supported by the National Natural Science Foundation of China (No. 20905010), the Ministry of Education Key Laboratory of Life Analytical Chemistry, funded projects for 2008 open issues of Nanjing University (No. KLACLS08007), the Changshu Municipal Science and Technology Agency-funded projects of China (No. CS200808), the Changshu Institute of Technology (Thesis) team issue funded projects of China.

Copyright © 2010, Changchun Institute of Applied Chemistry, Chinese Academy of Sciences. Published by Elsevier Limited. All rights reserved.

DOI: 10.1016/S1872-2040(09)60074-8

2.1 Apparatus and reagents

Myoglobin (Mb) was purchased from Beijing Shu Bo Wei Chemicals Instruments Co., Ltd, (Shanghai Branch, No. M1882). Other reagents were of analytical reagent grade. All solutions were prepared with double-distilled water. A saturated calomel electrode (SCE) and GE were purchased from Institute of Soil Science, Chinese Academy of Sciences. Electrochemical workstation (CHI660C) was purchased from Shanghai Chenhua Instrument Company. TU-1901 double-beam UV spectrophotometer was purchased from Beijing Purking General Instruments Co. Ltd., China. Fourier Transform Infrared (Vector 22 FT-IR) spectra spectrometer was purchased from Bruker Company. Scanning Electron Microscope (LEO, Electron Microscopy Ltd) was made in Germany.

2.2 Electrode preparation

Nickel oxide preparation was carried out according to the method described in literature^[15]. The solution preparation was as follows: A, 2.0 g L⁻¹ Mb water solution; B, 4.0 g L⁻¹ NiO dimethyl sulfoxide (DMSO) suspension; and C, 4.0 g L⁻¹ NiO water solution.

The modified GEs (geometric area: 0.2641 cm²) were polished before experiment with abrasive paper for metallograph (WAW7, 05) and 0.05- μ m α -alumina slurry (Beuhler), respectively, rinsed thoroughly with double-distilled water between each polishing step, sonicated in acetone and rinsed with double-distilled water successively and allowed to dry at room temperature.

Six prepared electrodes were as follows: (1) Bare electrodes, no analogs; (2) NiO/DMSO/GE, 5 μ L B and 10 μ L water; (3) Mb/GE, 10 μ L A and 5 μ L water; (4) Mb/NiO/GE, 10 μ L A and 5 μ L C; (5) Mb/DMSO/GE, 10 μ L A and 5 μ L DMSO; (6) Mb/NiO/DMSO/GE, 10 μ L A and 5 μ L B. A small bottle was fit tightly over the electrode for 2 h to ensure the slow evaporation of water and the formation of more uniform film. The film was then dried and aged overnight in a sealed flask kept at a constant temperature of 18 °C. Before the electrochemical experiments, the six electrodes were rinsed thoroughly with double-distilled water and kept in pH 7.0 PBS at 4 °C.

2.3 Measurements

Electrochemical measurements were performed on a CHI 660C electrochemical workstation (CHI Co., China) at (18 \pm 0.2) °C with a conventional three-electrode system with the modified GE as

working electrode, a platinum wire as auxiliary electrode, and an SCE as reference against which all potentials were measured. The stability of Mb/NiO/DMSO/GE was tested by increasing the temperature electrolysis pool, keeping the corresponding temperature 20 min and recording the cyclic voltammetry figure of methods. All experimental solutions were deoxygenated by bubbling highly pure nitrogen for 15 min and maintained under nitrogen atmosphere during measurements. The amperometric experiments were carried out by applying a potential of -350 mV on a stirred cell. The biosensor response was measured as the difference between total and residual currents.

UV-Vis absorbance spectroscopy was performed using TU-1901 double-beam UV spectrophotometer. Fourier transform infrared (FT-IR) spectra were recorded on a Vector 22 FT-IR spectrometer (Bruker). Mb solution, Mb/DMSO solution, Mb/NiO/water, or Mb/NiO/DMSO suspension were cast on a Teflon chip respectively. After the membrane on the chip was dried in air, it was stripped off and tabletted with KBr powder for FT-IR measurement. Twenty scans were collected and averaged for each spectrum. After modifying NiO, Mb and Mb/NiO/DMSO on a glassy slice respectively, these films were examined under a scanning electron microscope.

3 Results and discussion

3.1 Spectroscopic analysis of Mb/NiO/DMSO film

Figure 1 shows the UV-Vis spectra of different solution systems. The research indicates that Soret absorption band of myoglobin in solutions is in 409 nm^[16], so it is very significant that the absorption peak in Fig.1 is myoglobin's Soret absorption band in solution. The migration or disappearance of absorption band suggests changes in protein structure^[17,18]. Thus, the Mb mixed in the suspensions of NiO/DMSO, NiO/water, pure DMSO, and water could retain its native structure.

As well known, the shapes of infrared absorption bands of amide I and amide II in Mb molecule can provide detailed information on the secondary structure of the polypeptide chain. The absorption band of 1600–1700 cm⁻¹ for amide I is caused by C=O stretching vibration of peptide linkages in the protein's backbone. The absorption band around 1500–1620 cm⁻¹ for

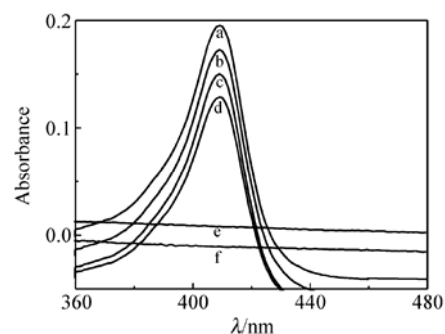


Fig.1 UV-Vis spectra of Mb/NiO/DMSO (a), Mb/DMSO (b), Mb/NiO (c), Mb (d), NiO/DMSO (e), and DMSO (f) solutions

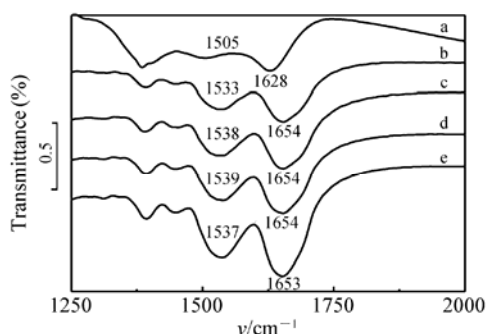


Fig.2 FT-IR spectra of NiO (a), Mb/DMSO (b), Mb (c), Mb/DMSO (d), and Mb/NiO/DMSO (e) films

amide II is resulted from a combination of N–H bending and C–N stretching. The loss of activity in Mb will eliminate the distinctive absorption bands of amide I and amide II^[19,20]. Figure 2 shows FT-IR spectra. The absorption bands for amide I and amide II in the Mb/NiO/DMSO film were nearly the same as those obtained for the protein itself. Both FT-IR and UV-Vis spectroscopic experiments suggested that the Mb in Mb/NiO/DMSO film was not grossly denatured and retained its native structure.

3.2 SEM characterization

Figure 3 shows the SEM images of NiO, Mb, and Mb/NiO/DMSO. It can be seen that the Mb molecules mixed with NiO particles are smaller and dispersed, and the electron transfer more fully between Mb and electrodes because of the dispersion of NiO nano-particles and reduction in the accumulation of Mb serious agglomeration.

3.3 Direct electrochemistry of Mb/NiO/DMSO-modified electrode

Figure 4 shows the cyclic voltammograms of different electrodes in 0.1 M pH 7.0 phosphate buffer solution. The Mb/NiO/DMSO/GE gave a couple of stable and well-defined redox peaks at -0.3677 and -0.3127 V at 100 mV s^{-1} (curve f), while no redox peak was observable in curves a and b. Obviously, the

response of the Mb/NiO/DMSO/GE was attributed to the redox of the electroactive centers in the immobilized Mb. However, the peak current of curve f was much bigger than curves c and d. Thus, the presence of DMSO played an important role in accelerating the electron transfer between Mb and the electrode. It was because of the decrease of the dielectric constant of the microenvironment around protein molecules, which decreased the reorganization energy of biological electron transfer, thus accelerated the electron transfer in protein^[19]. It was also because of the electronic exchange of the active site relatively exposed, promoting direct electron transfer. However, the peak current curve f was 2 times higher than curve e, thus, NiO nanoparticles were more important for facilitating the electron exchange. NiO nanoparticles provided a three-dimensional stage and some of the restricted orientations also favored the direct electron transfer between the protein molecules and the conductor surface. However, NiO nanoparticles could be strong adsorption, so the electrode had more Mb, and during the electrode processing, it was difficult to get rid of Mb, so the signal became large.

The formal potential E^0 of the heme Fe(III)/Fe(II) couple in Mb/NiO/DMSO/GE, estimated as the midpoint of anodic and cathodic peak potentials, was -0.34 V at pH 7.0 PBS. With an increasing scan rate, the anodic and cathodic peak potentials of the Mb showed small shift and the redox peak currents increased linearly, which indicated a surface-controlled electrode process. The electron transfer rate constant k_s was estimated according to model of Laviron formula $k_s = mnFv/RT$ to be $6.48 \text{ s}^{-1[20]}$, where m is a parameter related to the peak-to-peak separation. From the integration of the reduction peaks of the Mb/NiO/DMSO/GE at different scan rates, an average surface coverage of Mb (Γ) was calculated to be $8.06 \times 10^{-10} \text{ mol cm}^{-2}$, which indicated a high load of enzyme molecules.

3.4 Effect of solution pH on direct electron transfer of Immobilized Mb

In pH 5–10, the formal potential and solution pH is a linear relationship, with a slope of -42.3 mV per pH ($R = 0.9993$), which was close to $43.9 \text{ mV} \cdot \text{pH}^{-1[21]}$ and the expected value of $-57.8 \text{ mV} \cdot \text{pH}^{-1}$ at 291 K, indicating that one proton participated in the electron transfer process^[22]. The pH 7.0 PBS buffer solution was the experiment electrolyte because the highest peak current value appeared in pH 7.0 PBS solution.

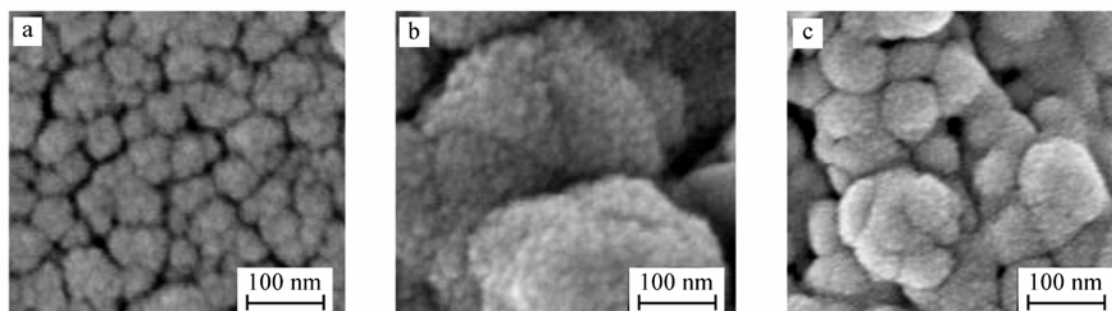


Fig.3 Scanning electron micrographs of NiO (a), Mb (b), and Mb/NiO/DMSO (c) films on a glassy slice

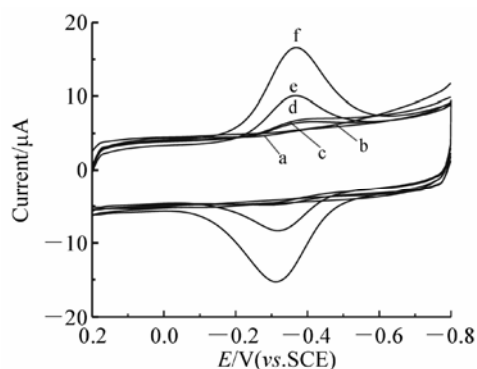


Fig.4 Cyclic voltammograms of GE (a), NiO/DMSO/GE (b), Mb/GE (c), Mb/NiO/GE (d), Mb/DMSO/GE (e), and Mb/NiO/DMSO/GE (f) in 0.1 M pH 7.0 PBS at 100 mV s⁻¹

3.5 Electrocatalysis of Mb/NiO/DMSO/GE to H₂O₂

Upon addition of H₂O₂ to the electrochemical cell in pH 7.0 PBS, the reduction peak current increased and the anodic peak current dramatically decreased. This phenomenon was not observed at a bare GE or a NiO/DMSO/GE electrode. Thus, the catalytic reduction of H₂O₂ was due to the presence of Mb, and the catalytic effect was very obvious. Figure 5 shows the amperometric response of the Mb/NiO/DMSO/GE at an applied potential of -350 mV on successive additions of H₂O₂ to a stirring 0.1 M pH 7.0 PBS. Upon addition of an aliquot of H₂O₂ to the buffer solution, the reduction current increased steeply to reach a stable value. The modified electrode achieved 95% of the maximum steady-state current in less than 5 s. This demonstrated clearly that the electrocatalytic response was very fast. So it can be used for rapid detection of H₂O₂. The linear response range of the sensor to H₂O₂ concentration was from 0.8 to 24 μM under the optimum conditions. The limit of detection was estimated to be 0.039 μM at a signal-to-noise ratio of 3σ from the slope. The enzymatic saturation response was observed (not be expressed)

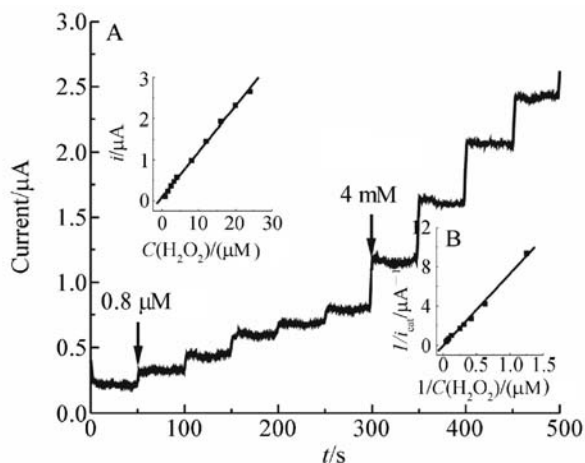


Fig.5 Amperometric response of the sensor at -350 mV on successive additions of H₂O₂ in pH 7.0 PBS at 100 mV s⁻¹. Inset: plot of catalytic current vs. H₂O₂ concentration (A) and the Lineweaver-Burk plot (B)

when the concentration of H₂O₂ was higher than 24 μM, which showed a characteristic of the Michaelis-Menten kinetic mechanism. The apparent Michaelis-Menten constant (K_M^{app}) of Mb/NiO/DMSO-modified electrode for H₂O₂ was obtained to be 0.21 mM from the electrochemical version of the Lineweaver-Burk equation. The K_M^{app} value was much smaller, thus, Mb modified by NiO had a high affinity to H₂O₂. The Mb/NiO/DMSO-modified electrode showed a sensitivity of 417 mA M⁻¹ cm⁻² to H₂O₂, which was much higher than 97 mA M⁻¹ cm⁻² for Mb in zirconia nanoparticles enhanced grafted collagen (ZrO₂-grafted collagen) hybrid composite^[16].

3.6 Thermal stability of Mb/NiO/DMSO/GE

The immobilization of proteins and enzymes onto transducer surfaces can lead to a change of their behavior compared with that observed in homogeneous solution^[21,23]. Thermal stability is a measure of the ability of the biosensor to withstand elevations in temperature^[24]. Both the anodic and cathodic peak currents of the Mb/NiO/DMSO/GE increased with increasing temperature from 15 to 85 °C, displaying an expected Arrhenius-type temperature dependence. Meanwhile, no peak was observed at the Mb/GE up to 50 °C, indicating the loss of Mb^[25]. The increase in the thermal stability of the Mb/NiO/DMSO/GE could be attributed to the presence of NiO nanoparticles. The immobilized Mb on hydrophobic NiO nanoparticles could greatly enhance the thermal stability because of the unusual conformational rigidity in this nonpolar binding environment.

3.7 Stability and reproducibility of Mb/NiO/DMSO-modified electrode

When it was cyclically swept between -0.8 and +0.2 V in 0.1 M pH 7.0 PBS at for 100 times, the peak current measurements corresponding to the direct electrochemistry of the immobilized Mb gave a relative standard deviation of 0.887%. So NiO was very efficient for retaining the oxidation and reduction activity of immobilized Mb and preventing it from leaking out of the biosensor, indicating a good repeatability. This sensor could retain 94.0% of its initial current response after 60-day storage in 0.1 M pH 7.0 PBS at 4 °C, showing better stability.

References

- [1] Ozaki S, Matsui T, Roach M P, Watanabe Y. *Coord. Chem. Rev.*, **2000**, 198(1): 39–59
- [2] Rusling J F. *Acc. Chem. Res.*, **1998**, 31(6): 363–369
- [3] Zhou Y, Hu N, Zeng Y, Rusling J F. *Langmuir*, **2002**, 18(10): 211–219
- [4] Collinson M M, Howells A R. *Anal. Chem.*, **2000**, 72(21): 702A–709A

- [5] Lvov Y M, Lu Z, Schenkman J B, Zu X, Rusling J F. *J. Am. Chem. Soc.*, **1998**, 120(17): 4073–4080
- [6] Zhao J, Henkens R W, Stonehuerner J, O'Daly J P, Crumbliss A L. *J. Electroanal. Chem.*, **1992**, 327(1-2): 109–119
- [7] Xiao H Y, Ju H X, Chen H Y. *Anal. Biochem.*, **2000**, 278(1): 22–28
- [8] Liu S Q, Ju H X. *Electroanalysis*, **2003**, 15(18): 1488–1493
- [9] He P L, Hu N F. *Electroanalysis*, **2004**, 16 (13-14): 1122–1131
- [10] Liu S Q, Leech D, Ju H X. *Anal. Lett.*, **2003**, 36(1): 1219
- [11] Willner I, Willner B, Katz E. *Bioelectrochemistry*, **2007**, 70(1): 2211
- [12] Xiao Y, Ju H X, Chen H Y. *Anal. Chem.*, **2000**, 60(20): 2263–2268
- [13] Shipway A N, Lahav M, Willner I. *Adv. Meterol.*, **2000**, 12(13): 993–998
- [14] Yang J X, Li Z H, Gao D S, Su G Y. *Fine Chemical Intermediates*, **2003**, 33(6): 53–64
- [15] Liu J H, Yu M, Li S M. *Journal of Materials Engineering*, **2006**, 21: 110–116
- [16] Zong S Z, Cao Y, Zhou Y M, Ju H X. *Biosens. Bioelectron.*, **2007**, 22(8): 1776–1782
- [17] Nassar A-E F, Willis W S, Rusling J F. *Anal. Chem.*, **1995**, 67(14): 2386–2392
- [18] Song Y P, Petty M C, Yarwood J, Feast W J, Tsibouklis J, Mukherjee S. *Langmuir*, **1992**, 8(1): 257–261
- [19] Zhou H X. *J. Am. Chem. Soc.*, **1994**, 116(23): 10362–10375
- [20] Laviron E. *J. Electroanal. Chem.*, **1979**, 101(1): 19–28
- [21] Weetall H H. *Anal. Chem.*, **1974**, 46(7): 602A–612A
- [22] Sun H, Hu N F, Ma H Y. *Electroanalysis*, **2000**, 12(13): 1064–1070
- [23] Bowers L. *Anal. Chem.*, **1986**, 58(4): 513A–530A
- [24] Wang J, Liu J, Cepra G. *Anal. Chem.*, **1997**, 69(15): 3124–3127
- [25] Liu S Q, Dai Z H, Chen H Y, Ju H X. *Biosens. Bioelectron.*, **2004**, 19(9): 963–969

研究报告

DOI: 10.3724/SP.J.1096.2010.01533

肌红蛋白在氧化镍纳米粒子中的固定
及新型生物传感器的制备宗水珍¹ 崔荣静¹ 费蕾¹ 李巍巍¹ 鞠焯先^{* 2}¹(常熟理工学院化学与材料工程学院,常熟 215500)²(南京大学化学化工学院生命分析化学教育部重点实验室,南京 210018)

摘要 研究了在氧化镍纳米粒子改性石墨电极(GE) 上肌红蛋白(Mb) 的直接电化学行为,并制备了新型 H₂O₂ 传感器。在 0.1 mol/L 磷酸盐缓冲溶液(PBS, pH 7.0) 中,肌红蛋白有稳定而明确的氧化还原峰,电子转移速率常数为 6.48/s; 式量电位为 -0.34 V(vs · SCE), 表面覆盖量 8.06 × 10⁻¹⁰ mol/cm²。二甲亚砜(DMSO) 的存在对加速肌红蛋白分子与电极之间的电子传递起了重要作用。光谱分析表明: 固定在 Mb/NiO/DMSO 膜中肌红蛋白能保持其生物活性,对 H₂O₂ 有电催化活性,电催化响应与 H₂O₂ 浓度呈线性关系,线性范围为 0.8 ~ 24 μmol/L; 检出限为 0.039 μmol/L。对 H₂O₂ 的表现米氏常数为 0.21 mmol/L,灵敏度为 417 mA cm² L/mol,呈现出高亲和性。

关键词 氧化镍纳米粒子; 生物传感器; 过氧化氢; 肌红蛋白; 电子转移

1 引言

研究蛋白质和酶的直接电化学和电催化,对于认识生命体内的电子转移机制和酶的催化机理以及重要生命物质在生命体内的代谢过程有着重要意义^[1]。近期研究表明,利用表面活性剂^[2,3]、溶胶-凝胶膜^[4]、离子聚合物^[5]、纳米材料^[6~11]等通过包埋、交联、组装等形式将血红素蛋白质固定在电极表面,可以实现血红素蛋白质与电极的直接电子传递。随着纳米材料性质研究的深入,蛋白质(酶)分子在纳米粒子上的固定研究也备受关注^[6,12,13]。肌红蛋白(Mb) 表现出的生理功能及参与的代谢过程,大多数涉及电子传递过程,它是研究血红素类蛋白质的直接电化学以及生物传感和电催化的理想模型。氧化镍(NiO) 作为一种功能材料,对其功能开发及应用研究都非常活跃^[14]。

本研究以 NiO 纳米粒子修饰石墨电极表面固定肌红蛋白分子,考察了蛋白质在此电极上的直接电化学行为,设计选择性、稳定性及重现性均佳,且准确、可靠、方便、灵敏的新型第 3 代生物传感器。

2 实验方法

2.1 仪器与试剂

饱和甘汞电极、石墨电极(中国科学院南京土壤研究所研制); CHI660C 电化学工作站(上海辰华仪器公司); TU-4901 双光束紫外可见分光光度计(北京普析通用仪器有限责任公司); 扫描电子图像分析仪(德国 Gemini 公司); Vector 22 FT-IR 傅立叶红外光谱(Bruker 公司)。

M1882 肌红蛋白(Mb, 北京舒伯伟化工仪器有限责任公司上海分公司) 其它试剂均为分析纯,水为二次蒸馏水。

溶液 A: 2.0 g/L Mb 水溶液; 溶液 B: 含 4.0 g/L NiO 的二甲亚砜(DMSO) 悬浮液; 溶液 C: 4.0 g/L NiO 水溶液。

2010-03-18 收稿; 2010-06-11 接受

本文系国家自然科学基金(No. 20905010)、南京大学“生命分析化学教育部重点实验室”2008 年度开放课题项目(No. KLACLS08007)、常熟市科技局项目(No. CS200808) 及常熟理工学院毕业设计(论文) 团队课题项目资助

* E-mail: hxju@nju.edu.cn

2.2 电极制备

氧化镍的制备参见文献 [15]。

改性石墨电极 (GE) 的面积为 0.2641 cm^2 , 实验前先在 WAW7(05) 金相砂纸上打磨, 再用 $0.05 \mu\text{m}$ 氧化铝在麂皮上打磨呈镜面, 每次抛光前都必须将电极用二次蒸馏水充分冲洗, 抛光结束后依次用丙酮和二次蒸馏水超声清洗 5 min , 最后在室温下晾干。

制备 6 种电极: (1) 裸电极: 不加修饰物; (2) NiO/DMSO/GE 电极: $5 \mu\text{L B} + 10 \mu\text{L H}_2\text{O}$; (3) Mb/GE 电极: $10 \mu\text{L A} + 5 \mu\text{L H}_2\text{O}$; (4) Mb/NiO/GE 电极: $10 \text{ mL A} + 5 \mu\text{L C}$; (5) Mb/DMSO/GE 电极: $10 \mu\text{L A} + 5 \mu\text{L DMSO}$; (6) Mb/NiO/DMSO/GE 电极: $10 \mu\text{L A} + 5 \mu\text{L B}$ 放入干燥瓶中 2 h , 使水分缓慢挥发以形成均匀膜, 然后将电极置于恒温 $18 \text{ }^\circ\text{C}$ 的密封瓶中过夜, 干燥后即制得 6 种电极。将 6 种电极用二次蒸馏水冲洗干净, 在 $4 \text{ }^\circ\text{C}$ 、PBS (pH 7.0) 中保存待用。

2.3 测试方法

使用三电极系统, 修饰 GE 为工作电极, 铂丝为辅助电极, 饱和甘汞电极 (SCE) 为参比电极, 与 CHI660C 电化学工作站连接进行电化学测量, 无特别说明, 电位值均是相对于 SCE 的电位。循环伏安实验在恒温 (18 ± 0.2) $^\circ\text{C}$ 、静止的电化学电解池中进行。通过升高电解池温度并在相应温度处恒温 20 min , 记录循环伏安图的方法来考察 Mb/NiO/DMSO/GE 的稳定性。所有电化学测试在实验前均先通高纯氮 15 min 以除去电解液中溶解氧, 在整个实验过程中保持氮气氛围。安培检测时, 工作电位为 -350 mV , 催化电流是测得的电流和起始电流之差。

将 Mb 溶液、Mb/DMSO 溶液、Mb/NiO/H₂O 或 Mb/NiO/DMSO 的悬浮液分别滴加在聚四氟乙烯片上, 在空气中晾干后将膜揭下, 用 KBr 压片后测试。每次测量的图谱是收集 20 次扫描结果的平均值。分别将 NiO、Mb 和 Mb/NiO/DMSO 修饰在玻璃片上, 进行扫描电子图像分析。

3 结果与讨论

3.1 Mb/NiO/DMSO 膜的光谱分析

肌红蛋白在溶液中的 Soret 吸收带在 409 nm [16]。图 1 是不同溶液紫外-可见吸收光谱, 图中出现的吸收峰是肌红蛋白在溶液中的 Soret 吸收带。吸收带的迁移或消失表明蛋白质的结构发生变化 [17, 18]。本实验结果显示, 混合在 NiO/DMSO、NiO/水悬浮液、DMSO 和水中的肌红蛋白均能保持它的天然结构。

肌红蛋白分子中酰胺 I 和酰胺 II 红外吸收带能提供多肽链二级结构的信息。酰胺 I 的 $1600 \sim 1700 \text{ cm}^{-1}$ 吸收带是由蛋白质肽链骨架中的肽段连接处 C=O 伸缩振动引起, 酰胺 II 的 $1500 \sim 1620 \text{ cm}^{-1}$ 吸收带则产生于 N—H 弯曲振动和 C—N 伸缩振动, 当蛋白质失去活性后, 分子中酰胺 I 和酰胺 II 的两个特征吸收带将显著改变甚至消失 [18, 19]。在傅立叶红外光谱 (图 2) 中, Mb/NiO/DMSO 得到的结果很接近肌红蛋白酰胺 I 和酰胺 II 的吸收带数值。傅立叶红外和紫外可见吸收光谱实验都证明, 固定在 Mb/NiO/DMSO 膜中的肌红蛋白分子不容易失活并能保持它的天然结构。

3.2 修饰膜的扫描电镜图

图 3 为 NiO、Mb、Mb/NiO/DMSO 的扫描电子显微镜图。从图 3 可见, Mb 分子与 NiO 混合后颗粒明显变小且分散均匀, 这是由于 NiO 纳米粒子起到分散 Mb 的作用, 减少了 Mb 的严重堆积团聚现象, 使得 Mb 与电极之间的电子转移更加充分。

3.3 Mb/NiO/DMSO/GE 修饰电极的直接电化学

图 4 是不同电极的循环伏安图。Mb/NiO/DMSO/GE 在 -0.3677 和 -0.3127 V 处出现一对稳定、峰形对称的氧化还原峰 (曲线 f)。而在同样条件下, 曲线 a 和曲线 b 上未观察到任何氧化还原峰, 由此说明产生的响应由固定在电极上的肌红蛋白电活性中心的氧化还原反应引起。另一方面, 曲线 f 峰电流比曲线 c 和 d 大得多, 说明在电子传递过程中 DMSO 起了重要作用。原因是 DMSO 使肌红蛋白分子周围环境的双电层常数降低, 从而使蛋白质电子传递过程的外部重组能降低, 因而加速了蛋白质的电子传递 [20], 也有可能使电子交换活性中心相对外露, 促进直接电子传递。然而曲线 f 峰电流比曲线 e 大 2 倍, 故 NiO 纳米粒子对加速肌红蛋白的电子传递起了更重要的作用: NiO 纳米粒子可能提供一个三维

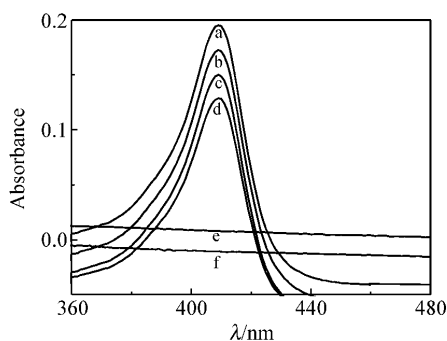


图 1 Mb/ NiO/DMSO(a) , Mb/DMSO(b) , Mb/NiO(c) , Mb(d) , NiO/DMSO(e) 和 DMSO(f) 溶液的紫外可见光谱图

Fig. 1 Uv-vis spectra of Mb/NiO/DMSO (a) , Mb/DMSO(b) , Mb/NiO(c) , Mb(d) , NiO/DMSO(e) and DMSO(f) solutions

Mb: Myoglobin; DMSO: Dimethylsulfoxide.

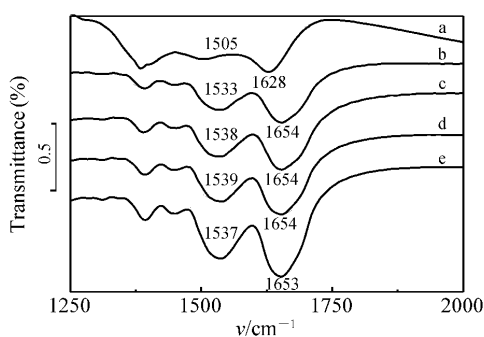


图 2 NiO(a) , Mb/NiO(b) , Mb(c) , Mb/DMSO(d) 和 Mb/NiO/DMSO(e) 的红外光谱图

Fig. 2 FT-IR spectra of NiO(a) , Mb/DMSO(b) , Mb(c) , Mb/DMSO(d) and Mb/NiO/DMSO(e) films

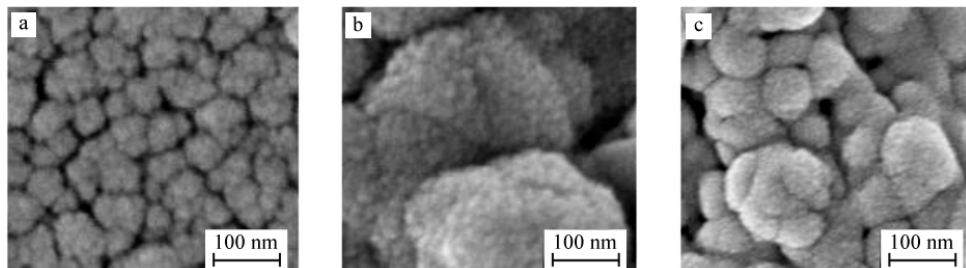


图 3 NiO(a) , Mb(b) 和 Mb/NiO/DMSO(c) 修饰在玻璃片上的扫描电镜图

Fig. 3 Scanning electron micrographs of NiO(a) , Mb(b) and Mb/NiO /DMSO (c) films on a glass slice

界面,使一些本来受到限制的方位也能适合蛋白质分子与电极表面之间的直接电子传递,从而加速电子传递过程;另外,NiO 纳米粒子吸附性强,吸附了更多的 Mb,且电极处理时难以洗脱,故信号大。

根据阳极与阴极峰电位的平均值求得,在 pH 7.0 时,Mb/NiO/DMSO/GE 上肌红蛋白中 $Fe^{3+/2+}$ 电对的式量电位 $E^{\theta} = -0.34$ V。随着扫速增加,肌红蛋白的阴极和阳极峰电位发生微小偏移,而峰电流则线性增加,说明是表面控制的电极反应过程。根据 Laviron 模型^[21],由公式 $k_s = mnFv/RT$ (m 是与峰电位差值有关的参数),求得电子转移速率常数 k_s 为 $6.48 s^{-1}$ 。通过对 Mb/NiO/DMSO/GE 电极在不同扫速下峰的整合,求得表面覆盖量为 $8.06 \times 10^{-10} mol/cm^2$,表明电极上蛋白分子的高载荷。

3.4 溶液 pH 值对肌红蛋白直接电子传递的影响

在 pH 5 ~ 10 范围内,式量电位与溶液 pH 值呈线性关系,斜率为 $-42.3 mV/pH$ ($r = 0.9993$),与 $-43.9 mV/pH$ ^[22] 接近,且接近于 291 K 时的理论值 $-57.8 mV/pH$,说明此过程是有一个质子和一个电子参与的电子传递过程^[23]。在 pH 7.0 时,峰电流值最高,故本实验中电解质溶液选择 PBS 缓冲体系 (pH 7.0)。

3.5 Mb/NiO/DMSO/GE 对 H₂O₂ 的电催化

Mb/NiO/DMSO/GE 在 PBS (pH 7.0) 中加入 H₂O₂ 后,还原峰电流显著增加,而氧化峰电流显著减小,在裸 GE 或 NiO/DMSO/GE 上未观察到此现象,说明 H₂O₂ 的催化还原是由于电极上存在有肌红蛋白分子,且催化效果明显。Mb/NiO/DMSO 修饰电极对 H₂O₂ 的安培响应见图 5。在 0.1 mol/L PBS (pH 7.0) 中连续加入适量 H₂O₂,选择 $-350 mV$ 作为工作电位,修饰电极对 H₂O₂ 显示良好的电催化活性,而且在 5 s 内可达到稳态电流的 95%,表明电催化响应很快,因此可用于 H₂O₂ 的快速检测。在最佳实验

条件下, H_2O_2 浓度的线性范围是 $0.8 \sim 24 \mu\text{mol/L}$; 从斜率可求得在信噪比为 3 时, 检出限是 $0.039 \mu\text{mol/L}$ 。当 H_2O_2 浓度大于 $24 \mu\text{mol/L}$ 时, 可观察到一个平台, 显示出 Michaelis-Menten 动力学机理的特征。表观米氏常数 K_{Mapp} 可以用 Lineweaver-Burk 方程求出, Mb/NiO/DMSO 修饰电极对 H_2O_2 的 K_{Mapp} 为 0.21 mmol/L 。此值较小, 说明氧化镍修饰的 Mb 对 H_2O_2 有很好的亲和性。此修饰电极的灵敏度为 $417 \text{ mA cm}^{-2} \text{ L/mol}$, 此值高于 Mb 修饰在接枝胶原 ZrO_2 复合材料中的灵敏度 ($97 \text{ mA cm}^{-2} \text{ L/mol}$)^[16]。

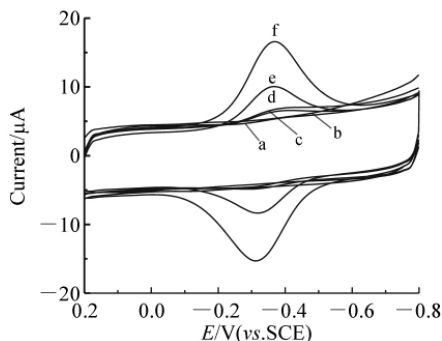


图 4 GE (a), NiO/DMSO/GE (b), Mb/GE (c), Mb/NiO/GE (d), Mb/DMSO/GE (e) 和 Mb/NiO/DMSO/GE (f) 在 0.1 mol/L PBS (pH 7.0) 中扫速为 100 mV/s 的循环伏安图

Fig. 4 Cyclic voltammograms of graphite electrode (GE) (a), NiO/DMSO/GE (b), Mb/GE (c), Mb/NiO/GE (d), Mb/DMSO/GE (e) and Mb/NiO/DMSO/GE (f) in 0.1 mol/L PBS (pH 7.0) at 100 mV/s

3.6 Mb/NiO/DMSO/GE 电极的热力学稳定性

固定在导电物质表面上的蛋白质或酶的行为与其在同相溶液中的行为相比会发生一些改变^[22-24]。热力学稳定性实验可检验生物传感器在电解液温度升高时的耐热性^[25]。在 $15 \sim 85 \text{ }^\circ\text{C}$ 范围内, 随着温度的升高, Mb/NiO/DMSO/GE 的阴极和阳极峰电流增加, 并呈现出理想的 Arrhenius 型温度依赖关系。而相同条件下, 当温度超过 $50 \text{ }^\circ\text{C}$ 时, Mb/GE 上肌红蛋白的氧化还原峰消失, 说明在此温度下固定在电极上的肌红蛋白分子已经失去活性^[26], 因此 Mb/NiO/DMSO/GE 的热力学稳定性增加的原因可归咎于 NiO 纳米粒子的存在, 由于在这种非极性键合环境中不寻常的刚性构象结构导致了固定在疏水性 NiO 纳米粒子表面的肌红蛋白的热力学稳定性极大地增加^[25]。

3.7 Mb/NiO/DMSO 修饰电极的重复性和稳定性

在工作电位 $-0.8 \sim 0.2 \text{ V}$ 之间, 将 Mb/NiO/DMSO/GE 在 PBS (pH 7.0) 中连续扫描 100 圈, 相对标准偏差为 0.887% , 重复性良好。修饰电极于 $4 \text{ }^\circ\text{C}$, PBS (pH 7.0) 中保存 60 d 后, 测得峰电流值为原来的 94% , 说明 Mb/NiO/DMSO/GE 具有良好的稳定性。

References

- Ozaki S, Matsui T, Roach M P, Watanabe Y. *Coor. Chem. Rev.*, **2000**, 198(1): 39 ~ 59
- Rusling J F. *Acc. Chem. Res.*, **1998**, 31(6): 363 ~ 369
- Zhou Y, Hu N, Zeng Y, Rusling J F. *Langmuir*, **2002**, 18(1): 211 ~ 219
- Collinson M M, Howells A R. *Anal. Chem.*, **2000**, 72(21): 702A ~ 709A
- Lvov Y M, Lu Z, Schenkman J B, Zu X, Rusling J F. *J. Am. Chem. Soc.*, **1998**, 120(17): 4073 ~ 4080
- Zhao J, Henkens R W, Stonehuerner J, O'Daly J P, Crumbliss A L J. *Electroanal. Chem.*, **1992**, 327(1-2): 109 ~ 119
- Xiao H Y, Ju H X, Chen H Y. *Anal. Biochem.*, **2000**, 278(1): 22 ~ 28
- Liu S Q, Ju H X. *Electroanal.*, **2003**, 15(18): 1488 ~ 1493
- He P L, Hu N F. *Electroanal.*, **2004**, 16(13-14): 1122 ~ 1131

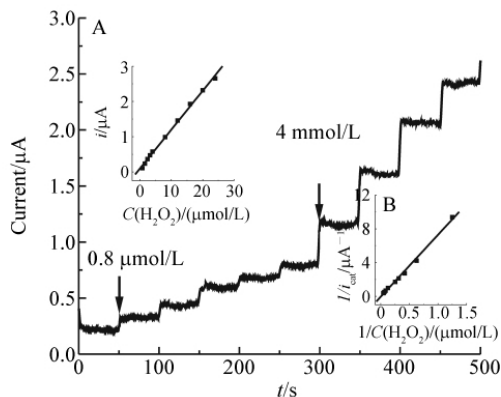


图 5 传感器在 pH 7.0 的 PBS 中电位为 -350 mV 时对 H_2O_2 的安培响应图

Fig. 5 Amperometric response of sensor at -350 mV upon successive additions of H_2O_2 in pH 7.0 PBS

插图 A 是电流对 H_2O_2 浓度的线性关系图, 插图 B 是 Lineweaver-Burk 图 (Inset: plot of catalytic current vs. H_2O_2 concentration (A) and the Lineweaver-Burk plot (B))。

- 10 Liu S Q , Leech D , Ju H X. *Anal. Lett.* , **2003** , 36(1) : 1219
- 11 Willner I , Willner B , Katz E. *Bioelectrochemistry* , **2007** , 70(1) : 2 ~ 11
- 12 Xiao Y , Ju H X , Chen H Y. *Anal. Chem.* , **2000** , 60(20) : 2263 ~ 2268
- 13 Shipway A N , Lahav M , Willner I. *Adv. Meterol.* , **2000** , 12(13) : 993 ~ 998
- 14 YANG Jian-Xiang(杨建湘) , LI Zhao-Hui(李朝晖) , GAO De-Shu(高德淑) , SU Guang-Yao(苏光耀) . *Fine Chemical Intermediates*(精细化工中间体) , **2003** , 33(6) : 53 ~ 64
- 15 LIU Jian-Hua(刘建华) , YU Mei(于美) , LI Song-Mei(李松梅) . *J. Mater. Engineer.* (材料工程) , **2006** , 21: 110 ~ 116
- 16 Zong S Z , Cao Y , Zhou Y M , Ju H X. *Biosens. Bioelectron.* , **2007** , 22(8) : 1776 ~ 1782
- 17 Nassar A E F , Willis W S , Rusling J F. *Anal. Chem.* , **1995** , 67(14) : 2386 ~ 2392
- 18 Song Y P , Petty M C , Yarwood J , Feast W J , Tsibouklis J , Mukherjee S. *Langmuir.* , **1992** , 8(1) : 257 ~ 261
- 19 Zhou H X. *J. Am. Chem. Soc.* , **1994** , 116(23) : 10362 ~ 10375
- 20 Laviron E. *J. Electroanal. Chem.* , **1979** , 101(1) : 19 ~ 28
- 21 Weetall H H. *Anal. Chem.* , **1974** , 46(7) : 602A ~ 612A
- 22 Sun H , Hu N F , Ma H Y. *Electroanalysis* , **2000** , 12(13) : 1064 ~ 1070
- 23 Bowers L. *Anal. Chem.* , **1986** , 58(4) : 513A ~ 530A
- 24 Wang J , Liu J , Cepra G. *Anal. Chem.* , **1997** , 69(15) : 3124 ~ 3127
- 25 Liu S Q , Dai Z H , Chen H Y , Ju H X. *Biosens. Bioelectron.* , **2004** , 19(9) : 963 ~ 969

Immobilization of Myoglobin on NiO Nanoparticles Matrix for Preparation of Novel Biosensor

ZONG Shui-Zhen¹ , CUI Rong-Jing¹ , FEI Lei¹ , LI Wei-Wei¹ , JU Huang-Xian^{* 2}

¹(Department of Chemistry and Material Engineering , Changshu Institute of Technology , Changshu 215500)

²(School of Chemistry and Chemical Engineering , Nanjing University , Key Lab of Analytical Chemistry for Life Science , Ministry of Education , Nanjing 210018)

Abstract Direct electrochemistry of myoglobin (Mb) immobilized on a nanometer-sized NiO nanoparticles matrix modified graphite electrode (GE) and preparation of novel hydrogen peroxide biosensor were studied. The immobilized Mb displayed a couple of stable and well-defined redox peaks with an electron transfer rate constant of 6.48 s^{-1} and a formal potential of -0.340 V (vs • SCE) in 0.1 mol/L PBS (pH 7.0) . The total surface concentration was $8.06 \times 10^{-10} \text{ mol/cm}^2$. Dimethyl sulfoxide (DMSO) could play an important role in the electron transfer between Mb and the electrode. Spectroscopy analysis of the Mb/NiO/DMSO film showed that the immobilized Mb could retain its natural structure. The electrocatalytic response showed a linear dependence on the H_2O_2 concentration ranging from 0.8 to 24 $\mu\text{mol/L}$ with a detection limit of 0.039 $\mu\text{mol/L}$ (3σ) . The apparent Michaelis Menten constant K_{Mapp} for H_2O_2 sensor was estimated to be 0.21 mmol/L and the sensitivity was $417 \text{ mA cm}^2 \text{ L/mol}$, which showed a high affinity.

Keywords Nickelous oxide nanoparticles; Biosensors; Hydrogen peroxide; Myoglobin; Electron transfer

(Received 18 March 2010; accepted 11 June 2010)